




Estimation of the addition of fly ash and its environmental impact in the manufacture of cement pastes

Juan D. Alonso¹ · Ximena Gaviria² · Julián E. López³ · Juan F. Saldarriaga^{1,2,4} 

Received: 13 July 2023 / Accepted: 5 February 2024
© The Author(s) 2024

Abstract

The cement industry is one of those that consumes the most energy, due to the high temperatures required to produce this material, and it is also one of the most that generates high CO₂ emissions. In this work, the addition of sugarcane ash, bituminous coal and hazardous residues in cement pastes were evaluated. For this, cement pastes were produced in accordance with ASTM C305, from which the test specimens were prepared to analyze compressive strength and parallel to this, metal leaching tests were performed using the SPLP procedure. Following this, the reactivity of the fly ash in the cement pastes was evaluated by means of thermogravimetric tests. The different analyzes were carried out at the ages of 1, 3, 7, 14, 28, 56, 90 and 180 days. The ashes were characterized by XRF, XRD, and laser grain size, where the SiO₂ and Al₂O₃ contents in the cane and bituminous coal ash were relatively high, contrary to what was obtained in the treated and untreated hazardous waste ash. These results are quite innovative because there are few works using HW in the literature. Cements with CAN, BIT, and THW5 were found to show equivalent and even superior compressive strength performance when compared to control. This work can be used as a guide and an inspiration for policymakers who want to apply this kind of material in the cement sector and promote evidence-based decisions and regulations.

Keywords Cement · Fly ash · Reactivity · Leaching test · Compressive strength

✉ Juan F. Saldarriaga
jf.saldarriaga@uniandes.edu.co; juanfernando.saldarriaga@ehu.eus

¹ Department of Civil and Environmental Engineering, Universidad de los Andes, Carrera 1Este #19A-40, Bogotá, Colombia

² Program of Industrial Engineering, Universidad de Medellín, Carrera 87 #30-40, Medellín, Colombia

³ Faculty of Architecture and Engineering, Institución Universitaria Colegio Mayor de Antioquia, Carrera 78 # 65-46, 050034 Medellín, Colombia

⁴ Department of Chemical Engineering, University of the Basque Country, B. Sarriena S/N, 49840 Leioa, Spain

1 Introduction

The significant increase in solid waste production has generated various environmental problems, including global warming, depletion of the ozone layer, threats to human health, damage to ecosystems, and depletion of natural resources. (Abdel-Shafy & Mansour, 2018; Papamarkou et al., 2018; Tantawy et al., 2012; Yusuf et al., 2019). The generation of municipal solid waste in urban areas in 2018 was approximately 2.01 billion metric tons per year (Ellis, 2019; Khandelwal et al., 2019), and by 2050, an increase of more than 50% in waste generation is expected, reaching almost 3.4 billion metric tons per year (Das et al., 2019; Margallo et al., 2019). By 2020 in Colombia, around 11.9 million tons of waste were generated, of which only 1.8% was used and only approximately 16% was recycled (Minambiente, 2022; Padilla & Trujillo, 2018). In the case of hazardous waste, according to the latest report from the Ministry of the Environment in 2019, around 640,000 tons were generated (IDEAM, 2020; Ordoñez-Ordoñez et al., 2019) and it is expected to continue to increase due to the emergence of new industries, regulatory compliance, and more controls (Arias Espana et al., 2018). The high generation of waste has led to sanitary landfills such as Doña Juana presenting disposal and management problems, causing water, soil, and air contamination (Bermudez et al., 2019; Giraldo et al., 2002).

Inadequate waste management has led developing countries to seek sustainability strategies (Das et al., 2019). The challenge is to find an integrated management of solid waste, which is focused from generation to disposal. The emphasis on waste management is linked to addressing the carbon footprint resulting from this activity. In the UK, landfills currently produce 14,446 tons of CO₂ equivalent annually, and it's projected to increase to 17,821 tons of CO₂ equivalent per year by 2030 (Clarke et al., 2019). Added to this is the fact that it has been reported that there is a relationship between urbanization and CO₂ emissions in developed countries, leading to solutions being proposed in which eco-innovations contribute to the reduction of environmental burdens (Aldieri et al., 2021a, 2021b). These solutions are associated with circular economy concepts, which involve the use of waste as raw materials in the manufacture of new eco-innovative products (Aldieri et al., 2021a, 2021b).

One of the alternatives that is easy and adequate for the management of waste, completely reducing its risk, is incineration (Papamarkou et al., 2018; Yang et al., 2018). One of the disadvantages of the incineration process is the generation of gases, fly ash and bottom ash. Ashes are considered hazardous waste due to the heavy metal content (Ghouleh & Shao, 2018; Papamarkou et al., 2018; Tantawy et al., 2012; Yang et al., 2018). Fly ash has elevated metal content caused by vaporization during incineration, potentially containing traces of various harmful compounds such as polycyclic organic compounds, PCBs, dioxins (Saikia et al., 2015), furans, and other contaminants (Kowalski et al., 2016). Other constituents that can be found in fly ash due to the toxic nature derived from heavy metals are Cd, Cr, Cu, Ni, Pb, and Zn (Stiernström et al., 2014). Fly ashes produced from incineration pose a disposal challenge as they cannot be deposited in regular sanitary landfills. In Colombia, the limited availability of secure landfills for such waste complicates its management (Aristizábal et al., 2008; Cobo et al., 2009).

As a result of this, in recent years, work has been carried out worldwide on the recovery of ashes, using different types, according to the residue incinerated. The estimated production of fly ash is around 800 million tons per year in the world (Tang et al., 2016; Toniolo & Boccaccini, 2017). Some of the main applications that have been found for this type of ash have been for its use as mineral additions to cements, concretes, and mortars;

also for road construction (Papamarkou et al., 2018; Saikia et al., 2015; Yang et al., 2018), and in the use of structures (Ginés et al., 2009; Rajamma et al., 2009; Saikia et al., 2015).

Cement industry is one of those that contributes the greatest proportion to CO₂ emissions (Chowdhury et al., 2015; Dong et al., 2015; Soyinka et al., 2023). The environmental reports of some cement companies such as Cemex and LafargeHolcim reveal that their emissions are between 561 and 622 kg of CO₂ per ton of cement produced (Fennell et al., 2021). Similarly, it has been determined that the amount of energy required for the production of one ton of cement is around 4 GJ (Elmrabet et al., 2019), making the process expensive. The use of supplementary materials can promote the sustainability of the cement industry, decreasing production costs and, therefore, the carbon footprint (Hassan et al., 2023; Moghaddam et al., 2019; Siddique, 2013; Soyinka et al., 2023). Different studies have been carried out on the application of fly ash and other materials, such as plastic, as well as alternative fuels in cement production (Çankaya, 2020; Chen et al., 2023; Das & Shrivastava, 2023; Sharma, 2018). At the same time, it has been investigated how these materials can affect the physical and chemical properties of cement and concrete as such. Several authors have focused on studying the chemical composition of different types of mineral additions to understand how they can function as cement substitutes (Bahurudeen et al., 2015; Jafari & Sadeghian, 2023; Saccani et al., 2017). Indicators have been established, such as the Si/Al ratio (Prošek et al., 2019; Wang et al., 2023), that show evidence that when making substitutions with mineral additions, pozzolanic reactions can occur, which are strongly influenced by the particle size (Moghaddam et al., 2019).

Most research has focused on the use of different types of ashes in order to evaluate whether better characteristics are evident than in cements and concretes (Prošek et al., 2019; Siddique et al., 2012). Replacement percentages between 10 and 30% by weight of ashes from different types of biomass with adequate mechanical properties have been found (Chusilp et al., 2009; Khan & Ali, 2019; Morales et al., 2021; Rodríguez-Fernández et al., 2020). Additionally, it has been shown that a high percentage of substitution contributes to the decrease in resistance (Morales et al., 2021; Prošek et al., 2019). Fly ashes from different types of biomasses, such as palm oil, rice husk, sugarcane bagasse, as well as bituminous coal, have been investigated, and it has been reported that up to 10% replacement shows the formation of CHS gels. In addition, compression resistance values are very similar to those of the control (Al-Kutti et al., 2019; Morales et al., 2021, 2023; Saldarriaga et al., 2022). On the other hand, fly ash from hazardous waste incineration processes in the manufacture of lime pastes has also been evaluated, finding that replacements of up to 5% can react and form CSH gels (Saldarriaga et al., 2022). A problem with the use of this type of ash is the possible metals they may contain, which is why there is little research on reactivity in the literature because the work has focused on encapsulation processes. Instead, it has been reported that the chemical composition of the mineral addition has a direct impact on the durability of the cement, as they can favor cement hydration reactions (Cho et al., 2019), but they can also be affected by the organic and inorganic impurities of the mineral additions, retarding or inhibiting them (Saikia et al., 2015). This can cause the structural properties of the cement to be affected as its age increases. For this reason, in this work the addition of fly ash to the manufacture of cylinder-shaped cement pastes has been evaluated by substitution with four types of fly ash (sugarcane, bituminous coal, treated and untreated hazardous waste) at various percentages in mass at different study times. In the first place, the reactivity of the mixtures was analyzed through thermogravimetric analysis, both standard and high resolution, to determine the phases present during the hydration process in the ash–cement matrices. Following that, the compression strength of the cylindrical pastes was evaluated. In order to assess the cement's ability to encapsulate heavy metals,

leaching experiments have been carried out on the produced cylinders, along with a control sample. This work is distinctive in that it looks at the correlation between the results of leaching tests and high-resolution TGA analyses carried out on different combinations. By using this technique, it has been noted that as CSH gels form in the cement pastes, the leaching of metals gradually reduces. This study validated the correlation between the specimens' mechanical strength and the potential degradation stages of the hydrated calcium silicates. Most importantly, these results demonstrate how extensively fly ash from hazardous trash was used in this investigation.

2 Materials and methods

The fly ash used in this work came from incineration processes. The sugar cane ashes were obtained from the Ingenio Carmelita, located in the municipality of Riofrío, Valle del Cauca. The coal ashes come from the company Conceniza S.A.S. from the city of Medellín, Antioquia, and the ashes from hazardous waste have been donated by the company Tecniamsa, a hazardous waste incineration plant located in the municipality of Mosquera, Cundinamarca. At Tecniamsa, the hazardous waste that undergoes incineration is electronic, hospital, and waste with hydrocarbon content, among others. The composition of this waste changes since the daily feed to the incineration furnace is different (CAR, 2009).

2.1 Pretreatment of hazardous waste ash

In accordance with Gene et al. (2019) and Saldarriaga et al. (2022), the hazardous waste ashes were washed in order to remove concentrations of salts, for example chlorides and/or sulfates (Saikia et al., 2015). For this, a water/ash ratio of 5:1 was taken (Gene et al., 2019; Saldarriaga et al., 2022). Subsequently, the sample was centrifuged at an acceleration of 10,000 g for one hour in order to settle the ashes. The supernatant was removed, and the precipitate was placed on trays and baked at 75 °C for 7 days to evaporate all the moisture content of the sample.

2.2 Characterization of the ashes

The chemical composition of the ashes was determined by X-ray fluorescence (XRF) carried out on Thermo brand wavelength equipment (Table 1). The mineralogical composition of the ashes was determined by X-ray diffraction (XRD) using a Miniflex-Rigaku X-ray diffractometer working with Bragg Brentano geometry, with CuK1.2 wavelength (1.54051 y 1.54433 Å) (Gene et al., 2019; Saldarriaga et al., 2022). The diffractometer was operated in the angular range of 2θ between 6 and 80°, using a step length of 0.02° and a time of two seconds per step.

Table 1 shows that for bituminous coal (BIT) and cane bagasse (CAN), the content of SiO₂, Al₂O₃, and Fe₂O₃ exceeds 70% (86.37% and 81.07%, respectively), therefore that can be classified as type F ash, according to ASTM C618 (ASTM, 2019). However, there are differences in the content of unburned material, which is 1.33% for BIT ash and 8.60% for CAN ash, allowing BIT ash to be classified as type F as pozzolans and CAN ash to be classified as type N because the content of CAN is close to the standard limit (ASTM, 2019), a result similar to that reported by other authors (Arenas-Piedrahita

Table 1 Chemical composition of the ashes obtained by XRF

Compound	Bituminous coal (BIT) wt%	Cane bagasse (CAN) wt%	Untreated hazardous waste (UHW) wt%	Hazardous waste treated (THW) wt%
SiO ₂	48.72	60.65	0.72	2.22
TiO ₂	–	0.80	0.05	0.24
Al ₂ O ₃	32.28	13.96	0.07	0.57
Fe ₂ O ₃	5.37	6.46	0.04	0.13
MnO	–	0.14	N.D	0.03
MgO	–	1.99	0.02	0.20
CaO	–	3.18	0.44	2.93
Na ₂ O	–	2.12	3.73	4.51
K ₂ O	–	1.53	0.37	0.37
P ₂ O ₅	–	0.35	0.04	0.25
SO ₃	1.04	0.03	1.32	3.25
Cl	–	–	4.27	3.23
ZnO	–	0.04	0.08	0.30
Cr ₂ O ₃	–	0.04	N.D	0.02
CuO	–	–	N.D	0.04
PbO	–	–	0.02	0.10
PPI (105°–1000 °C)	1.33	8.60	88.79	81.58
SiO ₂ + Al ₂ O ₃ + Fe ₂ O ₃ (%)	86.37	81.07	0.83	2.92
Si/Al mole ratio	1.28	3.70	8.01	3.31

et al., 2016; Cordeiro et al., 2009). Pozzolans have the ability to react with portlandite to form calcium hydrate silicates, which are mainly responsible for giving cement and concrete resistance (Teixeira et al., 2019; Wang et al., 2014), and class N ashes are considered as natural pozzolans that have appropriate requirements for any application or must be heat treated to improve their properties (ASTM, 2019).

In the same way, it can be observed that after washing the ashes of hazardous waste, the composition changes (Table 1). This is mainly due to the elimination of inorganic salts, followed by the possible reactions that occurred in the washing and centrifuging processes to which the sample has been subjected. Regarding the metal content, unlike coal ash, both sugarcane ash and untreated hazardous waste (UHW) and treated hazardous waste (THW) hazardous waste contain metals. These metals are in the form of oxides, which add up to 0.08%, 0.1, and 0.46%, respectively, percentages that exceed the limits allowed for residues that are considered non-hazardous (Gene et al., 2019).

Regarding the Si/Al ratio, similar values are evident between sugarcane ash and treated hazardous waste (3.70 and 3.31, respectively). For bituminous coal ash and untreated hazardous waste ash, the Si/Al ratios are widely scattered (1.28 and 8.01, respectively). The results of Duxson et al. (Duxson et al., 2007) indicate that good resistances can be obtained with Si/Al ratios between 1.15 and 1.90 and that, in the same way, as the Si/Al ratio increases, the structural properties improve. Riahi et al. (2020) found that as the Si/Al ratio increases, the amount of water required for good workability increases, and in turn, the strength may decrease.

Another factor to consider for mineral additions is the amount of unburned material. The higher the percentage of this material, the content of iron, silicon, and aluminum oxides decreases. This, in turn, affects the reactivity of the mineral addition, reducing the surface area and requiring more water, which leads to a decrease in the resistance of concrete (Arenas-Piedrahita et al., 2016).

2.3 Determination of particle size distribution

The determination of the particle size distribution by laser granulometry was carried out for type I cement and the four ashes (CAN, BIT, THW, and UHW) using a CILAS 1064 particle analyzer using the laser diffraction method. For this, isopropyl alcohol has been used as a dispersing agent in a range between 0.4 and 500 mm, according to the SM 2560D method of Standard Methods (Methods, 2018).

2.4 Monolith preparation

The cement and ash pastes were made in accordance with the ASTM C305 standard (American Society for Testing and Materials 2014). The ratio of water-cement and water-cementing material that has been used is 0.5 (Teixeira et al., 2019). The cement that was used for the preparation of the specimens was a gray cement for general use type I brand ARGOS (American Society for Testing & Materials, 2017; Argos, 2020). The cylinders were made with dimensions of 1 inch in diameter by 2 inches high. The strength specifications of the type I cement used in this study for day 3 is 8 MPa, day 7 is 15 MPa, and day 28 is 24 MPa (Argos, 2020).

The mixing proportions used in the manufacture of the pastes in which a greater reactivity was observed were obtained from the work carried out by Gene et al. (2019) and Saldarriaga et al. (2022). For mixtures with CAN and BIT, the replacement percentage was approximately 30%. In the case of UHW, a mixture of approximately 10% was used, while for THW, ratios in the range of 3–5% were used. The temperature and humidity conditions for the preparation of the specimens were followed in accordance with the ASTM C192 standard (American Society for Testing and Materials, 2018a). The finished cylinders were stored in a curing room at a temperature of 23 °C and a relative humidity of 95%. The pastes were stored in a container with water without direct contact, as described in the ASTM C511 standard (Arenas-Piedrahita et al., 2016; Committee, 2019).

2.5 Tests of resistance to compression of the specimens

The compressive strength tests of the specimens were carried out in accordance with the ASTM C39 standard (American Society for Testing and Materials, 2018b) at the ages of 1, 3, 7, 14, 28, 56, 90, and 180 days using an MTS universal machine, which uses a one-ton pump at a compression speed of 2 mm/min to determine the resistance to compression at the time the specimens fail. In order to accomplish this, three replicas were taken in line with the standard, brought to the universal MTS machine, and individually failed. These have been collected and then processed in accordance with the explanation provided in Sect. 2.6. On the day of each failure, all the specimens were removed from the curing room.

2.6 Thermal analysis using thermogravimetry (TGA)

For all the samples, thermogravimetric tests were carried out in order to analyze the phases present in the mixtures. The smallest fractions of the residues generated in the resistance tests were taken, and the hydration was stopped with acetone (Hewlett, 2004; Medina et al., 2018). It was vacuum filtered for 3–5 min, and the samples were placed in an oven at 60 °C for one hour (Velázquez et al., 2016). The already dry samples were crushed with a mortar and sieved through a 200 sieve of the ASTM-E series (opening 75 microns) in such a way that a fine powder was obtained (Ashraf et al., 2019). The samples were placed in Eppendorf tubes and taken to a desiccator for mounting in the thermogravimetric analysis equipment (TGA 5500, TA Instruments).

For thermogravimetric analysis, ultra-high purity nitrogen (UAP) was used as the inert atmosphere as purge gas. The heating range was established between 30 and 600 °C, and the heating ramp used was 10 °C/min up to 600 °C (Gaviria et al., 2018; Morales et al., 2023; Saldarriaga et al., 2022).

2.6.1 High resolution TGA thermal analysis

For pastes with a curing time of 180 days, high-resolution thermogravimetric analyzes were carried out. Since it was observed that the pozzolanic reactions increased in that period. The maximum temperature established for high-resolution tests was 300 °C with a heating ramp of 50 °C/min (Gaviria et al., 2018; Morales et al., 2021; Rodríguez-Fernández et al., 2020). In the program used for the high-resolution TGA analyses, different ratios of resolutions and sensitivities were tested in the TGA. Accordingly, a resolution of +5 and a sensitivity of 3 were established as the best relationship because, with these parameters, a better separation of the peaks included in a temperature range between 80 and 200 °C was observed, which corresponds to the decomposition of C–S–H gels and shows the phases formed in the process.

2.7 Leaching tests

The leaching test has been carried out on each of the days evaluated in the reactivity and compressive strength tests (1, 3, 7, 14, 28, 56, 90, and 180 days). To evaluate if at those moments there is a release of the metals present in the ashes and compare it with the other tests to determine if there were impacts to the environment on the evaluation days. For this, they have been taken two test tubes were taken from each mixture with ash, including the reference for the test. The use of sugarcane ash test tubes was not considered for the test since, according to their characterization, they did not present heavy metals (Table 1). The test was carried out using the synthetic precipitation leaching procedure (SPLP) (US EPA, 2015). The fluid used was water and a mixture of H₂SO₄/HNO₃ in a 60/40 wt% ratio, adjusting the pH to 4.2 ± 0.05 according to EPA Method 1312 (US EPA, 2015). The test tube was introduced into a bottle, and 250 ml of SPLP fluid was added; it was left to rest for 24 h. The fluid was then filtered into extraction flasks preserved with nitric acid for the reading of metals by ICP-OES.

2.8 Metal analysis by ICP-OES

For the analysis of metals by ICP-OES, a microwave-assisted acid digestion was performed with concentrated nitric acid and hydrochloric acid so that the metals remained dissolved in the sample and to be able to carry out the metal analysis according to EPA Method 3015 (US EPA, 2019). Digestion was carried out with nitric acid and hydrochloric acid at a temperature of 170 °C for 10 min. After cooling, the contents of the vial were filtered and diluted to volume with 5% v/v nitric acid (HNO₃) and then analyzed by ICP-OES (Inductively Coupled Plasma Atomic Emission Spectroscopy).

2.9 Scanning electron microscopy (SEM)

Scanning electron microscopy (SEM) tests were performed in order to observe the formation of C–S–H gels. Likewise, to be able to corroborate the data obtained through TGA. The experiments were conducted using a TESCAN LYRA3 FIB-SEM microscope (Tescan, Brn, Czech Republic). The samples have been analyzed after 180 days of curing for all the mixtures tested.

3 Results and discussion

3.1 X-ray diffraction to fly ash

Figure 1a–d show the diffractograms of the four fly ashes that were used for this work (CAN, BIT, UHW, and THW). It can be seen in the CAN and BIT ash diffractograms (Fig. 1a, b) that there are less intense patterns with respect to the UHW and THW diffractograms (Fig. 1c, d). This means that the CAN and BIT ashes present more amorphous compounds than the UHW and THW ashes, such as SiO₂, MgO, and Fe₂O₃. This aspect is favorable and desirable in hydration reactions (Memon et al., 2019), which influence the structural properties of cements. With this condition, it is expected that the amorphous phases can react with calcium hydroxide (Ca(OH)₂) for the formation of calcium hydrate silicates, showing that these mineral additions have pozzolanic behavior, influencing the properties of the concrete (Arenas-Piedrahita et al., 2016).

For UHW (Fig. 1c), intense diffraction patterns are shown at 32.08° and 45.78°, evidencing the existence of a crystalline phase of CaO and PbO, an inappropriate condition in mineral additions that decreases their capacity as substitutes for Portland cement (Memon et al., 2019). Although in THW (Fig. 1d) less intense peaks are shown, exhibiting amorphous characteristics, for that reason the pretreatment carried out on the ashes of hazardous waste could reduce the degree of crystallinity of the fly ash, an appropriate condition to favor the reactivity of these materials (Gene et al., 2019; Morales et al., 2023; Saldarriaga et al., 2022).

Compounds such as silicon dioxide were found, which was observed in the four diffractograms as amorphous phases because such intense peaks were not shown, according to the chemical composition of the ashes (Table 1). For the mineral addition of the CAN ash, compounds such as MnO₂ and MgSO₄ expressed as langbeinite were found (Saldarriaga et al., 2022). In the case of the BIT ash, compounds such as CaO, KAlSi₂O₆, and magneto-ferrite (MgFe₂O₄) were present (Kocak & Nas, 2014; Morales et al., 2023;

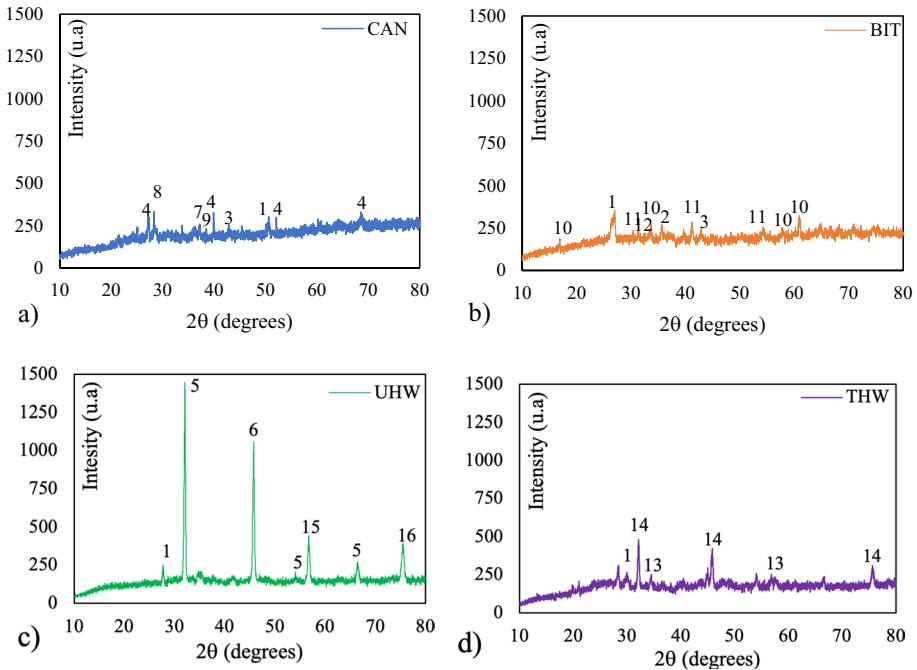


Fig. 1 Diffractograms of the four fly-ash analyzed **a** CAN ash, **b** BIT ash, **c** UHW ash, **d** THW ash. (1) SiO_2 , (2) Fe_2O_3 , (3) MgO , (4) TiO_2 , (5) CaO , (6) PbO , (7) $\text{Mg}_2\text{Al}_2\text{O}_4$, (8) $\text{K}_2\text{Mg}_2(\text{SO}_4)_3$, (9) CaSiO_3 , (10) Al_2SiO_5 , (11) Mg_2SiO_4 , (12) $\text{K}_2\text{Ca}_2(\text{SiO}_4)_3$, (13) $\text{Ca}_3\text{Al}_2\text{Si}_3\text{O}_{12}$, (14) NaCl , (15) Fe_3O_4 , (16) FeO

Saldarriaga et al., 2022). These ashes have high contents of silicon and aluminum oxides (Table 1), and according to what was reported by Arenas-Piedrahita et al. (2016) these could be considered mineral additions with pozzolanic properties in accordance with the specifications of the standard ASTM (ASTM, 2019), but only if they have significant reactivity.

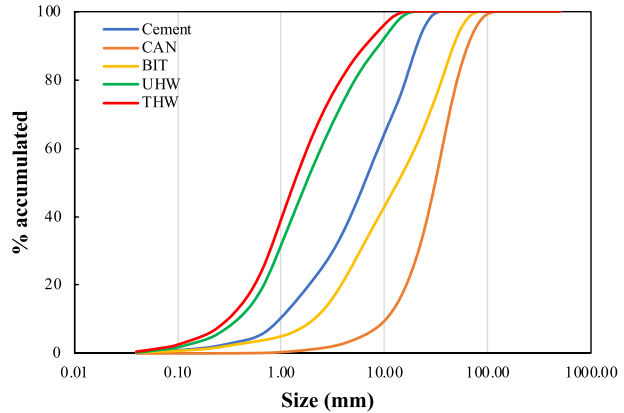
In UHW and THW, NaCl was found in quantities of approximately 4%, an aspect that, according to Saldarriaga et al. (2022), should not be greater than 0.6% to avoid alkali reactions, which produce aggregates over time that can cause the disintegration of the concrete.

In UHW, there are iron oxide compounds expressed as FeO , Fe_2O_3 , and Fe_3O_4 , which can favor the pozzolan reaction as reported by Arenas-Piedrahita et al. (2016), contributing to the hydration of the aluminosilicates, taking into account that the mineral additions must meet the requirement of aluminum, iron, and silicon oxides as described by ASTM (2019) to be used as a substitute for cement.

3.2 Particle size distribution

Figure 2 shows the cumulative distributions of particle sizes for the worked cement and the four fly ashes (CAN, BIT, THW, and UHW). Some similarities are observed in the distributions of the particle sizes of the UHW and THW ashes, where their sizes are below $10\ \mu\text{m}$, which represents a good condition to favor the reactivity of the ash with the cement

Fig. 2 Cumulative distribution of particle sizes for type I cement and the four ashes



(Bui et al., 2005; Xu et al., 2006). In contrast to the CAN and BIT particle size distributions, where the majority of the particles are greater than 10 μm , Arenas-Piedrahita et al. (2016) observed similar behavior. This results in heterogeneity, with some particles being larger than others, affecting the reactivity of these ashes and slowing pozzolanic reactions (Pavlíková et al., 2018).

The results shown in Table 2 clearly demonstrate that there is a difference in the average sizes of the four ashes in relation to the cement. The CAN and BIT ashes have larger mean sizes (34.70 and 19.76 μm , respectively), while the UHW and THW ashes have smaller mean sizes (3.26 and 2.49 μm). This size condition influences the reactivity because, as the particle size decreases, their surface area increases, favoring their ability to react with the cement (Darsanasiri et al., 2018). Therefore, hydration reactions are more favored, and better resistance can be developed (Darsanasiri et al., 2018; Qudoos et al., 2018). In fact, there is a big difference between the D_{90} of the CAN and BIT ashes with respect to the UHW and THW ashes. This size difference causes particles with a larger diameter than others to appear, which makes the particles less effective; their surface area is reduced; and the reaction of the pozzolans with the cement becomes slower (Pavlíková et al., 2018).

3.3 Tests of resistance to compression of the specimens

Figure 3 shows the evolution of the compressive strength of the specimens with the different ashes as their age increases. An increasing trend is shown as the age of the specimens increases. In the case of UHW substitution ashes, there were increases in resistance until day 7, and then there was a decrease in this resistance. These changes could be attributed

Table 2 Average size, D_{10} , D_{50} , and D_{90} , for the 5 samples obtained from laser granulometry

Particle type	Average size (mm)	D_{10} (mm)	D_{50} (mm)	D_{90} (mm)
Type I cement	8.93	0.98	6.48	20.69
CAN	34.70	10.39	31.15	64.40
BIT	19.76	2.11	13.54	46.93
UHW	3.26	0.38	1.77	8.87
THW	2.49	0.31	1.36	6.57

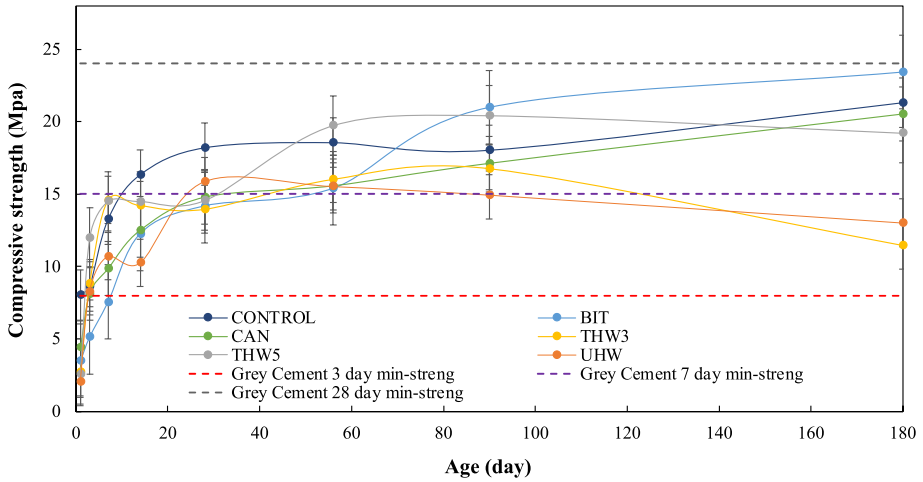


Fig. 3 Evolution of the compressive strength of the specimens with the different fly ash up to 180 days of age

to the heavy metal content of these ashes, which could have facilitated the formation of microcracks. These affected the formation of the hydration products, as shown in Fig. 4f, although the difference in resistance between days 7 and 14 of the UHW system was 0.45 MPa (Table 3), a difference that is not so significant. A collapse of the test tubes was observed between days 14 and 56, due to the microcracks generated by the metals in these hazardous waste ashes.

For the mixtures of CAN, BIT, Control, and THW5, a progressive increase in resistance was observed as the age of these specimens increased. The resistance was 4.41, 3.48, 8.03, and 2.56 MPa, respectively, for the mentioned systems (Table 3), while on day 28, the resistance was 14.78, 14.18, 18.20, and 14.55 MPa, respectively. This indicates that they have good structural properties to be used as inputs for construction. It is also observed that as the percentage of substitution of the ash of hazardous waste treated at 5% increases, the compressive strength decreases (Kaur et al., 2019). As the amount of ash in the cement matrix increases, the traces of heavy metals in the matrix will possibly increase (Ganesan et al., 2007), which can affect hydration reactions, as seen in Fig. 4d–f.

For the specimens made with CAN ash, an increasing trend in resistance similar to that reported by other authors was observed, although they used specimens of different dimensions (Sua-iam & Makul, 2013). For the specimens with BIT ash, an increase in resistance was observed (Nath & Sarker, 2011). This indicates that these ashes do have appealing properties for use as cement replacements because they improve their structural properties.

At later ages, for the control system, there were no significant variations in resistance between days 28 and 90; only until day 180 was there a variation close to 3 MPa in the resistance of the control system in relation to day 90, and the resistance reached a value of 21.32 MPa for this system at day 180 of hydration. At later ages, for the control system, there were no significant variations in resistance between days 28 and 90; only until day 180 was there a variation close to 3 MPa in the resistance of the control system in relation to day 90, and the resistance reached for this system a value of 21.32 MPa at day 180 of hydration (Arenas-Piedrahita et al., 2016). For the THW3 system, the

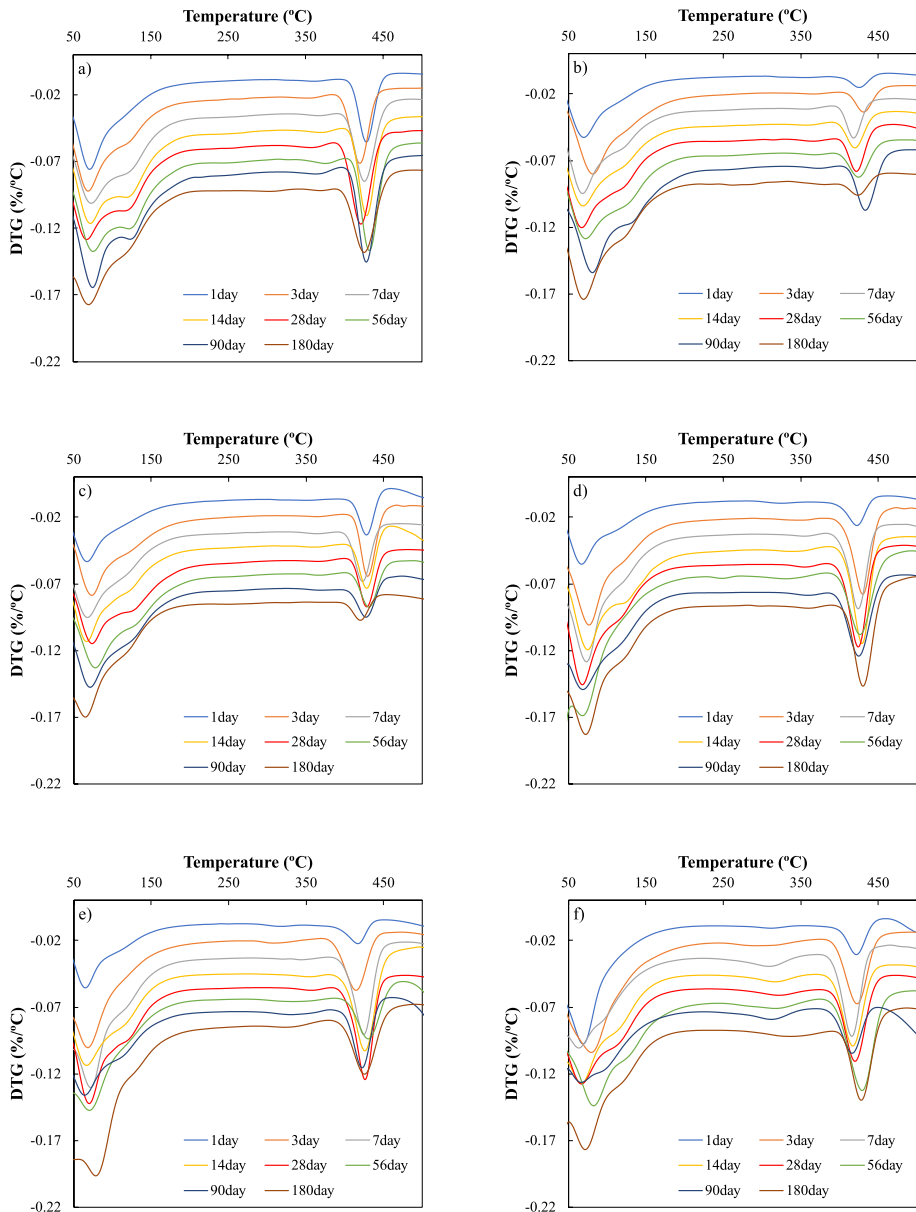


Fig. 4 Evolution of the formation of C-S-H gels as well as $\text{Ca}(\text{OH})_2$ for different days of hydration, **a** control, **b** cement-BIT ash, **c** cement-CAN ash, **d** cement-THW3, **e** cement-THW5, **f** Cement-UHW

maximum resistance was reached on day 90 at 16.77 MPa and decreased to 11.45 MPa, and for the UHW system, the maximum resistance was reached at 28 days with a value of 15.87 MPa and decreased progressively to a value of 13.02 MPa. Because the standard deviation for the UHW system is 4.65 MPa (Table 3), it can be assumed that the difference in resistance for days 28 and 180 of the UHW system is not significant, but

Table 3 Results of resistance tests for all systems up to 180 days of age

Age (day)	1	3	7	14	28	56	90	180	Standard deviation (MPa)
	Compressive strength (MPa)								
UHW	2.03	8.28	10.71	10.26	15.87	15.54	14.95	13.02	4.65
THW5	2.56	12.00	14.50	14.49	14.55	19.74	20.43	19.21	5.77
THW3	2.71	8.85	14.60	14.21	13.96	16.03	16.77	11.45	4.63
BIT	3.48	5.13	7.56	12.26	14.18	15.39	20.98	23.42	7.19
CAN	4.41	8.12	9.85	12.50	14.78	15.57	17.12	20.53	5.22
CONTROL	8.03	8.62	13.26	16.34	18.20	18.55	18.02	21.32	4.86

it shows that this resistance is not desirable. compared to the BIT, control, CAN, and THW5 systems.

For the systems with UHW and THW3, it was observed that, at early ages, the mixtures gained resistance in the same way as the BIT, CAN, THW5, and control systems. On day 1, the resistances for UHW and THW3 were 2.03 and 2.71 MPa, and on day 28, they were 15.87 and 13.96 MPa, thanks to the particle size of these ashes (Table 2). According to what was previously described, they could consume the portlandite faster because its surface area increased, causing greater reactivity in the ash (Darsanasiri et al., 2018; Qudoos et al., 2018).

In fact, in the TGA results of the mixtures with hazardous waste ash, pronounced peaks are observed at early hydration ages (Fig. 4d–f), but in turn, at late ages for the THW3 and UHW mixtures, a loss of resistance was observed, probably due to the content of heavy metals and other elements such as chlorine (Table 1). These metals may have aided in the formation of microcracks, which may have affected the structural properties of mixtures (Termkhajornkit et al., 2009).

3.4 Thermogravimetric analysis

Figure 4 shows the evolution of the cement hydration process as the age of the pastes increases; this is a representative characteristic of what occurred in all the mixtures studied. It is also possible to show an increase in the region characteristic of the decomposition of the different types of C–S–H gels, a region between 80 and 200 °C (Darsanasiri et al., 2018; Pavlíková et al., 2018; Teixeira et al., 2019). Keeping in mind that these silicates can occur in different forms and are not easily identifiable (Song et al., 2018), as well as the evolution in the amount of portlandite as the age of the specimens increased. A tendency to increase the content of Ca(OH)₂ was observed. What may be happening is that when mixed with fly ash containing silicon and aluminum oxides, it would lead to a pozzolanic reaction that could result in the formation of C–S–H and probably C–A–S–H (Saldarriaga et al., 2022), which translates into a positive effect on the quality of cements since hydrated calcium silicates contribute to their structural properties (Nakanishi et al., 2016).

For all systems, a similar behavior can be observed in terms of the decomposition of hydrated calcium silicates as the hydration time increases. The BIT and CAN mixtures with respect to the blank present similar behavior in terms of the decomposition region of the portlandite between 400 and 460 °C (Pavlíková et al., 2018). It is observed that a greater amount of portlandite decomposes at day 180 of hydration for these three

systems, although comparing the BIT and CAN graphs against those of cement, the portlandite decomposition peak is less pronounced with respect to the control since, due to its properties, it can react with calcium hydroxide to form hydrated calcium silicates (Pavlíková et al., 2018).

For the mixtures with UHW and THW ashes, a similar behavior is observed compared to the BIT, CAN, and control systems. Although in the case of THW3 and THW5, there is evidence of a reduction in the portlandite peak after 28 days of hydration with respect to day 14 of curing. This could give rise to a pozzolanic reaction as the portlandite may be transforming into some type of C–S–H phase (Chusilp et al., 2009). For the later ages (56, 90, and 180 days), very pronounced C–S–H and portlandite decomposition peaks are observed in all systems except the BIT and CAN systems. This could indicate that, in effect, with the use of mineral additions in concrete, they do not develop resistance at an early age but rather at a later age (Arenas-Piedrahita et al., 2016).

Figure 5 shows the evolution of the hydration process for all systems at 180 days of age. For all systems except the cement system with BIT ash and CAN ash, the formation of C–S–H gels in the region between 60 and 150 °C is very noticeable, as is the formation of portlandite in the temperature range between 350 and 450 °C. For the 30% BIT and CAN systems, what may be happening is that the reaction kinetics of the BIT ash and CAN ash with the cement are slow, which translates into a low formation of both C–S–H and portlandite (Jassam et al., 2019; Lenormand et al., 2015). For the system with THW5, it is observed that the portlandite decomposition peak is not so pronounced, due to the interaction of the ash with the portlandite for the formation of hydrated calcium silicates (Qudoos et al., 2018; Tang et al., 2016).

3.5 High resolution thermogravimetry tests

Figure 6 shows the decomposition process of the C–S–H gels for all systems after 180 days of curing. At this age, the best decomposition of C–S–H gels was evident. This is to see which phases of C–S–H are the ones that are being formed. It is observed that for all systems, there is a peak in the region between 40 and 70 °C. In the case of the control, there is a second peak in the region between 105 and 130 °C (Song et al., 2018). Mainly, the phases that may be forming are C–S–H and hydrated calcium aluminosilicates (Song et al., 2018). The hydrated calcium aluminosilicates correspond to gypsum or ettringite, phases that, as

Fig. 5 Total mass lost for a given temperature interval (DTG) for all systems after 180 days of hydration

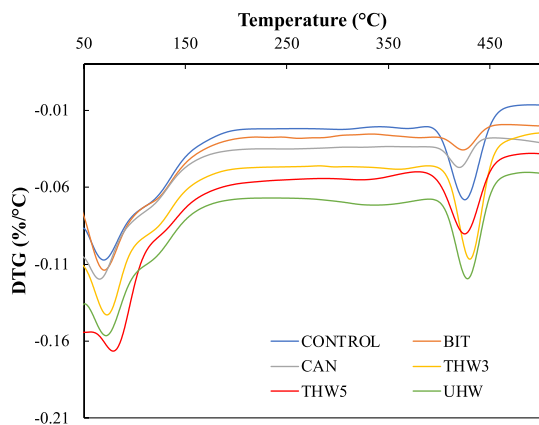
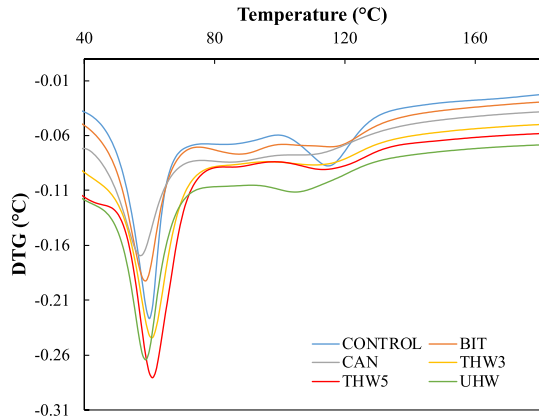


Fig. 6 Total mass lost for a determined temperature interval (DTG) in high resolution for all systems at 180 days of age



described by other authors (Arenas-Piedrahita et al., 2016), contribute to the reactions of the ashes with the portlandite to form the different types of C–S–H.

3.6 Leaching analysis

Tables S1–S4 show the results of the evolution of the concentration of heavy metals obtained by ICP from the leaching tests. The metals analyzed were Al, Ca, Cu, Mg, K, Na, Zn, Cr, Fe, Mn, and Pb. For all the mixtures analyzed, it is shown that there was a decreasing trend in the concentration of heavy metals in the leaching fluid. This suggests that as the hydration age of the pastes increased, the concentration of heavy metals increased because more chemical bonds could have been formed between the heavy metals and the calcium hydrate silicates formed during cement hydration reactions. This could have increased the encapsulation capacity of the ash–cement matrices, due to the formation of less reactive and more thermodynamically stable hydration products (del Valle-Zermeño et al., 2014) and therefore the leaching decreased. Table 4 shows the concentration of metals for the samples analyzed by leaching on day 180 of curing. It is evident that of the metals that are

Table 4 Concentration of heavy metals for the BIT, UHW and THW samples at day 180

Analyzed metal	Concentration (mg/L)			
	BIT	UHW	THW3	THW5
Aluminum	–	0.574	0.155	–
Calcium	–	193	178	196
Copper	–	–	–	–
Magnesium	–	0.14	0.152	0.158
Potassium	2.4	63.4	29.4	49.8
Sodium	7.48	–	126	209
Zinc	–	–	–	–
Chromium	–	–	–	–
Iron	–	–	–	–
Manganese	–	–	–	–
Lead	–	–	–	–

regulated both in Colombia and in other countries (Table S5), only the aluminum in the UHW is above the norm, while the remaining metals comply with the standard. Metals such as Mg, K, and Na are not legislated in water and soil; therefore, their leaching does not imply any risk to ecosystems in accordance with the legislation.

As shown in Tables S1–S4, there is a decreasing trend in heavy metal concentrations. Because as the cylindrical pastes hydrated, more chemical bonds were possibly formed between the metals and the calcium hydrate silicates, which probably prevented the release of the heavy metals from the three-dimensional ash–cement matrix. It is taken into account that the tolerance of the iCAP 6500 DUO equipment is between 0.001 and 10,000 mg/L according to the SM3120B method (Baird et al., 2017). In fact, it is observed that for the four systems analyzed (Tables S1–S4), there were days where the ICP detected some metals such as Pb, Al, and Fe and others where the equipment did not detect them. This can be attributed to an interference, either due to the impurities that the hazardous waste ashes had (Table 1) or due to the calibration of the equipment, but in the case of aluminum and iron, most of the concentrations were below the target. detection limit of the SM3120B method (Baird et al., 2017).

On days 14 and 28 of the BIT system for aluminum, the concentrations were 0.282 and 0.516 mg/L (Table S1), which exceed the water quality standard for Colombia (Table S5). It is possible that while the cylindrical pastes were hydrating, the ash compounds formed microcracks, allowing heavy metals to be released into the leach fluid (Termkhajornkit et al., 2009).

In the case of the UHW, THW3, and THW5 systems (Tables S2–S4), a decreasing trend is also observed in most of the metals analyzed. Some metals, such as Al, Na, Mg, and Fe, had their concentrations in the leaching fluid decrease as the age of the pastes increased until day 14, but on day 28, the concentrations of metals such as Al, Ca, Mg, and Fe increased (Tables S3, S4). This can be attributed to the fact that this type of ash that comes from hazardous waste incineration processes can generate a reaction with water due to the pretreatment carried out. In turn with the impurities, which could affect the hydration reactions of the pastes and the formation of calcium hydrate silicates for the immobilization of metals (Memon et al., 2019; Saikia et al., 2015).

In the case of Ca, its concentration in the UHW, THW3, and THW5 systems was above 100 mg/L on all test days, which indicates that it does not react with the cement and is not encapsulated either. However, this metal, according to the legislation, is not considered dangerous (Andrea Truque, 2012a).

For metals such as Cr and Pb, a decrease in their concentration was observed as the age of the pastes increased, a behavior similar to that shown by other authors (Xu et al., 2006). For the mixtures with UHW ashes (Table 4), it was observed that the Cr concentration was 0.185 mg/L at the time of carrying out the leaching test after 24 h of hydration of the pastes, and a progressively decreasing trend was observed until day 56, where the concentration obtained was 0.023 mg/L. At the ages of 90 and 180 days, the Cr concentrations obtained were below the detection limits of the EPA method 3015A and the SM 3120B method of the Standard Methods (Baird et al., 2017).

For the mixtures with THW3 and THW5 (Tables S3, S4), a trend similar to that observed in metals such as Cr and Pb is observed in the mixture with UHW ashes. Indeed, this indicates that during the hydration process, hydrated calcium silicates were formed (Fig. 4d–f), which allowed for less heavy metal leaching (Ginés et al., 2009). This has been observed at day 180 for these metals (Tables S3, S4). In fact, it is observed that the concentrations, despite the fact that some are exceeding the detection limit of the SM 3120B method of Standard Methods (Baird et al., 2017), are also very close to

the permitted limits of heavy metals (Table S5), which indicates the effectiveness of the ash–cement matrix for the immobilization of heavy metals.

3.7 SEM analysis

Figure 7 shows the images obtained from a scanning electron microscopy (SEM) analysis for all the replacements analyzed. The micrographs show the formation of crystals after 180 days of curing. In Fig. 7a and b, SEM images for CAN are shown at lengths of 200 and 50 μm , respectively. In Fig. 7b, the formation of crystals is clearly seen, which was also observed in the HR-TGA analyzes (Fig. 6), indicating the high reactivity observed during the entire curing time of the samples. Similarly, in Fig. 7c, the SEM analysis for the replacement with BIT is shown, in which, as with CAN, there is a high level of reactivity, and the TGA results are corroborated. Figure 7d shows the results for UHW, showing the formation of CSH gels that were presented in both the TGA and HR-TGA analyses. In the case of THW replacements (Fig. 7e, f), crystals are observed in both samples, but in THW3 there are more crystals than in THW5. With this, the TGA results are corroborated, and it is concluded that the THW3 sample shows reactivity results. A larger replacement could affect both the properties of the structure and favor the release of possible metals that are present in the fly ash. These results show that all types of ashes used in this study are of great interest for the construction industry, especially in developing countries such as

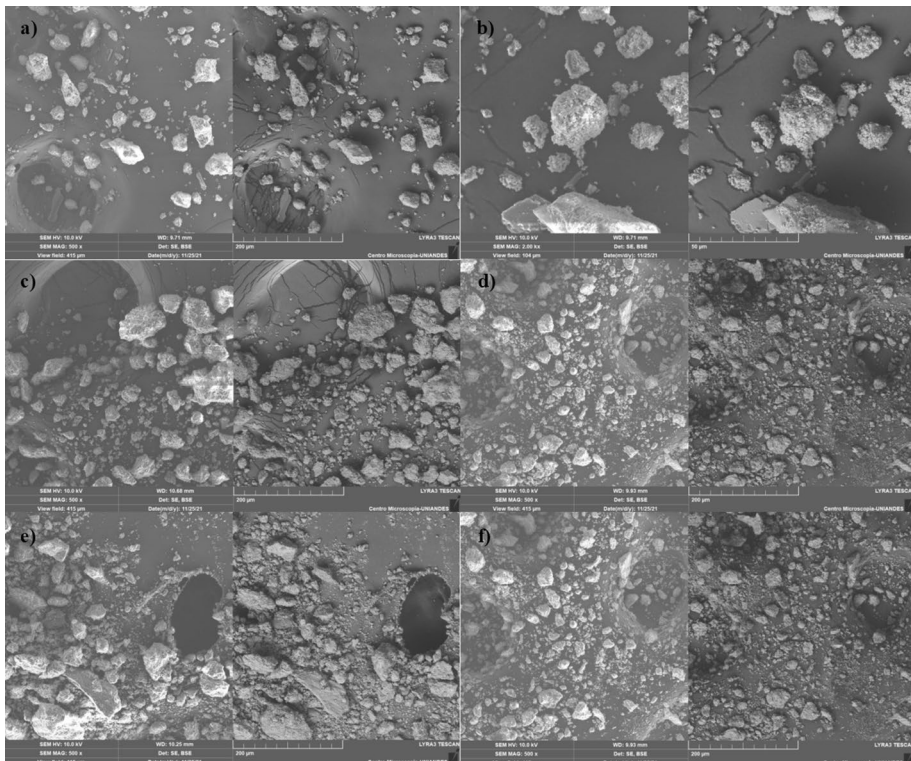


Fig. 7 Scanning electron microscope (SEM) for all replacements performed at day 180

Colombia, where this type of waste is deposited in landfills. With the use of fly ash in the construction industry, a significant contribution is made to the circular economy, especially in this industry, thereby reducing environmental impacts such as the effects on water, soil, and air.

The results of this research show that the replacement of fly ash in different proportions and depending on the type of ash can cause positive effects in the manufacture of low-performance inputs. These findings could suggest support for industrial innovation where a competition structure is developed, which, according to other authors, can reduce the negative externalities of innovation in the common environment and the impact of the innovation activities of the company on productivity (Aldieri et al., 2021b). These types of implementations could result in greater economic growth. With respect to policymakers and the construction industry, such as the establishment of special funds to encourage the use of this type of material in the industry, in order to be able to expand innovation activities. Likewise, it is necessary for construction company owners to increase investment in R&D, improving productivity and reducing the reliability of the dissemination of knowledge (Aldieri et al., 2021a, 2021b).

The results of this study significantly contribute to the sustainable development objectives upon which many developing countries have relied on their medium- and long-term sustainability goals. These results represent a significant step forward in addressing the environmental challenges related to solid waste management, particularly in handling and disposing of fly ash, which presents difficulties. The industrial application resulting from this research and initiative not only involves government and local actors but also integrates a diverse range of interested stakeholders and innovators. This integration aims to bring about changes in the dynamics of both the construction industry and sanitization company. Additionally, it contributes to the understanding of sustainability in two crucial economic sectors essential for fostering sustainable cities' development.

4 Conclusions

After analyzing the results of thermogravimetry, compressive strength, and leaching of the THW3, THW5, UHW, BIT, CAN, and control systems up to day 180 of age, it is concluded that the best mass ratios for its use in low-performance inputs are: cement with sugarcane ash, bituminous coal, and treated hazardous waste. The compressive strength tests showed that the strength increased as the age of the specimens increased. In the case of the UHW and THW3 systems, a different resistance behavior was found in relation to the other systems, mainly due to the variations in UHW between days 7 and 14. On day 7, a greater resistance is seen compared to day 14 of UHW. This is because at these ages, a collapse of the test tubes was observed, which affected their resistance.

In the late ages, an improvement in resistance was observed due to the reaction of the pozzolans with the portlandite, for the CAN, BIT, and THW5 systems, where the resistance was close to 23 MPa at 180 days of age. In the UHW and THW3 systems, the maximum strength reached was close to 15 MPa, which is a good strength compared to the control, which was approximately 21 MPa. This indicates that these materials are attractive for use as cement replacements. For THW3, the resistance was lower than THW5, since collapse of the specimens was observed on day 180, as in the UHW system. These resistance behaviors are related to the TGA analyses, where it was evidenced that there were more pronounced decomposition peaks of C–S–H and portlandite as the ages of the pastes

increased, which confirms that if these phases were formed, they were responsible for the strength of Portland cement. In turn, the high-resolution thermogravimetric analyzes showed that at the age of 180 days, the decomposition peak of the C–S–H became more noticeable, and when relating it to the compressive strength tests, an increasing trend in strength was indeed observed. to compression. In the same way, the leaching analyzes showed that the leaching of heavy metals was lower, at 180 days of age in relation to day 1. Which confirmed that for most metals analyzed the immobilization treatment is effective except for calcium, although this metal is not considered dangerous, according to the legislation.

These findings hold significance for both public policymakers and construction industry professionals. They reaffirm the suitability of utilizing this waste material as a cement substitute in the production of low-performance construction materials. However, more studies are necessary where these results are applied to real-scale tests in order to verify their good behavior, thus seeking to improve knowledge in this area, which can be applied at a business level.

With the above, it is proven that the mass ratios of BIT, CAN, and THW5 are adequate for the manufacture of low-performance inputs, such as bricks, bollards, pots, and paving stones, with the possibility of a study for the manufacture of sidewalks with a low flow of people.

Supplementary Information The online version contains supplementary material available at <https://doi.org/10.1007/s10668-024-04615-4>.

Acknowledgements This work was carried out with the support of the Department of Civil and Environmental Engineering at Universidad de Los Andes. The authors thank the team of technicians from the Environmental Engineering Research Center for the support provided during the development of this work. Juan D. Alonso thanks to the Department of Civil and Environmental Engineering for her teaching assistance scholarship.

Funding Open Access funding provided by Colombia Consortium.

Data availability The datasets generated during and/or analyzed during the current study are available from the corresponding author on reasonable request.

Declarations

Conflict of interest None.

Open Access This article is licensed under a Creative Commons Attribution 4.0 International License, which permits use, sharing, adaptation, distribution and reproduction in any medium or format, as long as you give appropriate credit to the original author(s) and the source, provide a link to the Creative Commons licence, and indicate if changes were made. The images or other third party material in this article are included in the article's Creative Commons licence, unless indicated otherwise in a credit line to the material. If material is not included in the article's Creative Commons licence and your intended use is not permitted by statutory regulation or exceeds the permitted use, you will need to obtain permission directly from the copyright holder. To view a copy of this licence, visit <http://creativecommons.org/licenses/by/4.0/>.

References

- Abdel-Shafy, H. I., & Mansour, M. S. M. (2018). Solid waste issue: Sources, composition, disposal, recycling, and valorization. *Egyptian Journal of Petroleum*, 27(4), 1275–1290. <https://doi.org/10.1016/j.ejpe.2018.07.003>

- Aldieri, L., Brahmi, M., Bruno, B., & Vinci, C. P. (2021a). Circular economy business models: The complementarities with sharing economy and eco-innovations investments. *Sustainability*, *13*(22), 12438. <https://doi.org/10.3390/su132212438>
- Aldieri, L., Brahmi, M., Chen, X., & Vinci, C. P. (2021b). Knowledge spillovers and technical efficiency for cleaner production: An economic analysis from agriculture innovation. *Journal of Cleaner Production*, *320*, 128830. <https://doi.org/10.1016/j.jclepro.2021.128830>
- Al-Kutti, W., Saiful Islam, A. B. M., & Nasir, M. (2019). Potential use of date palm ash in cement-based materials. *Journal of King Saud University-Engineering Sciences*, *31*(1), 26–31. <https://doi.org/10.1016/j.jksues.2017.01.004>
- American Society for Testing and Materials. (2014). *ASTM C305–14 Standard practice for mechanical mixing of hydraulic cement pastes and mortars of plastic consistency* (Vol. 04). ASTM International. <https://doi.org/10.1520/C0305-14>
- American Society for Testing And Materials. (2017). *ASTM C1157/C1157M-17, Standard performance specification for hydraulic cement*. ASTM International. https://doi.org/10.1520/C1157_C1157M-17
- American Society for Testing and Materials. (2018a). *ASTM C192/C192M-18, Standard practice for making and curing concrete test specimens in the laboratory* (Vol. 04). ASTM International. https://doi.org/10.1520/C0192_C0192M-18
- American Society for Testing and Materials. (2018b). *ASTM C39/C39M-18, Standard test method for compressive strength of cylindrical concrete specimens*. ASTM International. https://doi.org/10.1520/C0039_C0039M-18
- Andrea Truque, P. B. (2012). Armonización de los estándares de agua potable en las Américas. *Organization for American States: Democracy for peace, security and Environment*. Retrieved March 4, 2020, from <https://www.oas.org/dsd/publications/classifications/Armoniz.EstandaresAguaPotable.pdf>
- Arenas-Piedrahita, J. C., Montes-García, P., Mendoza-Rangel, J. M., López Calvo, H. Z., Valdez-Tamez, P. L., & Martínez-Reyes, J. (2016). Mechanical and durability properties of mortars prepared with untreated sugarcane bagasse ash and untreated fly ash. *Construction and Building Materials*, *105*, 69–81. <https://doi.org/10.1016/j.conbuildmat.2015.12.047>
- Argos, G. (2020, January 26). Cemento gris uso general. Retrieved from <https://colombia.argos.co/Conoce-nuestros-productos/Cementos-de-Uso-General>
- Arias Espana, V. A., Rodríguez Pinilla, A. R., Bardos, P., & Naidu, R. (2018). Contaminated land in Colombia: A critical review of current status and future approach for the management of contaminated sites. *Science of the Total Environment*, *618*, 199–209. <https://doi.org/10.1016/j.scitotenv.2017.10.245>
- Aristizábal, B., Cobo, M., Hoyos, A., Montes de Correa, C., Abalos, M., Martínez, K., et al. (2008). Baseline levels of dioxin and furan emissions from waste thermal treatment in Colombia. *Chemosphere*, *73*, S171–S175. <https://doi.org/10.1016/j.chemosphere.2007.03.078>
- Ashraf, M. S., Ghouleh, Z., & Shao, Y. (2019). Production of eco-cement exclusively from municipal solid waste incineration residues. *Resources, Conservation and Recycling*, *149*, 332–342. <https://doi.org/10.1016/j.resconrec.2019.06.018>
- ASTM. (2019). *ASTM C618–19, Standard specification for coal fly ash and raw or calcined natural pozzolan for use in concrete*. *Annual Book of ASTM Standards*. ASTM International. <https://doi.org/10.1520/C0618-19>
- Bahurudeen, A., Kanraj, D., Gokul Dev, V., & Santhanam, M. (2015). Performance evaluation of sugarcane bagasse ash blended cement in concrete. *Cement and Concrete Composites*, *59*, 77–88. <https://doi.org/10.1016/j.cemconcomp.2015.03.004>
- Baird, R. B., Eaton, A. D., & Rice, E. W. (2017). Standard Methods for the Examination of Water and Wastewater. (W. E. F. American Public Health Association, American Water Works Association, Ed.). American Public Health Association. Accessed 28 June 2020
- Bermudez, J. F., Montoya-Ruiz, A. M., & Saldarriaga, J. F. (2019). Assessment of the current situation of informal recyclers and recycling: Case study Bogotá. *Sustainability*, *11*(22), 6342. <https://doi.org/10.3390/su11226342>
- Bui, D. D., Hu, J., & Stroeven, P. (2005). Particle size effect on the strength of rice husk ash blended gap-graded Portland cement concrete. *Cement and Concrete Composites*, *27*(3), 357–366. <https://doi.org/10.1016/j.cemconcomp.2004.05.002>
- Çankaya, S. (2020). Investigating the environmental impacts of alternative fuel usage in cement production: A life cycle approach. *Environment, Development and Sustainability*, *22*(8), 7495–7514. <https://doi.org/10.1007/s10668-019-00533-y>
- CAR. (2009). Resolución 2469 de 2009 que autoriza tratamiento térmico por incineración. Retrieved June 26, 2020, from <http://www.tecniamsa.com.co/licencias/2017/Resolucion-2469-de-2009.pdf>

- Chen, B., Zuo, Y., Zhang, S., de Lima Junior, L. M., Liang, X., Chen, Y., et al. (2023). Reactivity and leaching potential of municipal solid waste incineration (MSWI) bottom ash as supplementary cementitious material and precursor for alkali-activated materials. *Construction and Building Materials*, 409, 133890. <https://doi.org/10.1016/j.conbuildmat.2023.133890>
- Cho, Y. K., Jung, S. H., & Choi, Y. C. (2019). Effects of chemical composition of fly ash on compressive strength of fly ash cement mortar. *Construction and Building Materials*, 204, 255–264. <https://doi.org/10.1016/j.conbuildmat.2019.01.208>
- Chowdhury, S., Mishra, M., & Suganya, O. (2015). The incorporation of wood waste ash as a partial cement replacement material for making structural grade concrete: An overview. *Ain Shams Engineering Journal*, 6(2), 429–437. <https://doi.org/10.1016/j.asej.2014.11.005>
- Chusilp, N., Jaturapitakkul, C., & Kiattikomol, K. (2009). Utilization of bagasse ash as a pozzolanic material in concrete. *Construction and Building Materials*, 23(11), 3352–3358. <https://doi.org/10.1016/j.conbuildmat.2009.06.030>
- Clarke, C., Williams, I. D., & Turner, D. A. (2019). Evaluating the carbon footprint of WEEE management in the UK. *Resources, Conservation and Recycling*, 141, 465–473. <https://doi.org/10.1016/j.resconrec.2018.10.003>
- Cobo, M., Gálvez, A., Conesa, J. A., & Montes de Correa, C. (2009). Characterization of fly ash from a hazardous waste incinerator in Medellín, Colombia. *Journal of Hazardous Materials*, 168(2), 1223–1232. <https://doi.org/10.1016/j.jhazmat.2009.02.169>
- Committee, C. (2019). Specification for mixing rooms, moist cabinets, moist rooms, and water storage tanks used in the testing of hydraulic cements and concretes. ASTM International. <http://www.astm.org/cgi-bin/resolver.cgi?C511-19> <http://files/212/C01> Committee - Specification for Mixing Rooms, Moist Cabinets, Mo.pdf
- Cordeiro, G. C., Toledo Filho, R. D., Tavares, L. M., & Fairbairn, E. D. M. R. (2009). Ultrafine grinding of sugar cane bagasse ash for application as pozzolanic admixture in concrete. *Cement and Concrete Research*, 39(2), 110–115. <https://doi.org/10.1016/j.cemconres.2008.11.005>
- Darsanasiri, A. G. N. D., Matalkah, F., Ramli, S., Al-Jalode, K., Balachandra, A., & Soroushian, P. (2018). Ternary alkali aluminosilicate cement based on rice husk ash, slag and coal fly ash. *Journal of Building Engineering*, 19, 36–41. <https://doi.org/10.1016/j.jobe.2018.04.020>
- Das, S., Lee, S.-H., Kumar, P., Kim, K.-H., Lee, S. S., & Bhattacharya, S. S. (2019). Solid waste management: Scope and the challenge of sustainability. *Journal of Cleaner Production*, 228, 658–678. <https://doi.org/10.1016/j.jclepro.2019.04.323>
- Das, S. K., & Shrivastava, S. (2023). A comparative study on the mechanical and acid resistance characteristics of ambient temperature-cured glass waste and fly ash-based geopolymeric masonry mortars. *Environment, Development and Sustainability*, 25(11), 13399–13427. <https://doi.org/10.1007/s10668-022-02622-x>
- del Valle-Zermeño, R., Chimenos, J. M., Giró-Paloma, J., & Formosa, J. (2014). Use of weathered and fresh bottom ash mix layers as a subbase in road constructions: Environmental behavior enhancement by means of a retaining barrier. *Chemosphere*, 117, 402–409. <https://doi.org/10.1016/j.chemosphere.2014.07.095>
- Dong, B., Qiu, Q., Xiang, J., Huang, C., Sun, H., Xing, F., & Liu, W. (2015). Electrochemical impedance interpretation of the carbonation behavior for fly ash–slag–cement materials. *Construction and Building Materials*, 93, 933–942. <https://doi.org/10.1016/j.conbuildmat.2015.05.066>
- Duxson, P., Mallicoat, S. W., Lukey, G. C., Kriven, W. M., & van Deventer, J. S. J. (2007). The effect of alkali and Si/Al ratio on the development of mechanical properties of metakaolin-based geopolymers. *Colloids and Surfaces a: Physicochemical and Engineering Aspects*, 292(1), 8–20. <https://doi.org/10.1016/j.colsurfa.2006.05.044>
- Ellis, C. (2019, September 25). World Bank: Global waste generation could increase 70% by 2050. *Waste Dive*. Retrieved September 25, 2019, from <https://www.wastedive.com/news/world-bank-global-waste-generation-2050/533031/>
- Elmrabet, R., El Harfi, A., & El Youbi, M. S. (2019). Study of properties of fly ash cements. *Materials Today: Proceedings*, 13, 850–856. <https://doi.org/10.1016/j.matpr.2019.04.048>
- Fennell, P. S., Davis, S. J., & Mohammed, A. (2021). Decarbonizing cement production. *Joule*, 5(6), 1305–1311. <https://doi.org/10.1016/j.joule.2021.04.011>
- Ganesan, K., Rajagopal, K., & Thangavel, K. (2007). Evaluation of bagasse ash as supplementary cementitious material. *Cement and Concrete Composites*, 29(6), 515–524. <https://doi.org/10.1016/j.cemconcomp.2007.03.001>
- Gaviria, X., Borrachero, M. V., Payá, J., Monzó, J. M., & Tobón, J. I. (2018). Mineralogical evolution of cement pastes at early ages based on thermogravimetric analysis (TG). *Journal of Thermal Analysis and Calorimetry*, 132(1), 39–46. <https://doi.org/10.1007/s10973-017-6905-0>

- Gene, J. M., Gaviria, X., & Saldarriaga, J. F. (2019). Evaluation of fly ash reactivity from incineration of hazardous waste in lime pastes. *Chemical Engineering Transactions*, 75, 619–624. <https://doi.org/10.3303/CET1975104>
- Ghouleh, Z., & Shao, Y. (2018). Turning municipal solid waste incineration into a cleaner cement production. *Journal of Cleaner Production*, 195, 268–279. <https://doi.org/10.1016/j.jclepro.2018.05.209>
- Ginés, O., Chimenos, J. M., Vizcarro, A., Formosa, J., & Rosell, J. R. (2009). Combined use of MSWI bottom ash and fly ash as aggregate in concrete formulation: Environmental and mechanical considerations. *Journal of Hazardous Materials*, 169(1), 643–650. <https://doi.org/10.1016/j.jhazmat.2009.03.141>
- Giraldo, E., Caicedo, B., Yamín, L. E., & Soler, N. (2002). The landslide of Doña Juana Landfill in Bogota. A Case Study. In *Proceedings of the Fourth International Congress on Environmental Geotechnics (4th ICEG)*.
- Hassan, A., Arif, M., Shariq, M., Alomayri, T., & Pereira, S. (2023). Fire resistance characteristics of geopolymer concrete for environmental sustainability: A review of thermal, mechanical and microstructure properties. *Environment, Development and Sustainability*, 25(9), 8975–9010. <https://doi.org/10.1007/s10668-022-02495-0>
- Hewlett, P. C. (2004). *Lea's chemistry of cement and concrete (Fourth Edi)*. Elsevier science & Technology books.
- IDEAM. (2020). *Informe nacional de residuos o desechos peligrosos en Colombia, 2019* (p. 180). Bogotá: Institute of Hydrology, Meteorology and Environmental Studies. Retrieved November 28, 2022, from <http://www.ideam.gov.co/documents/51310/124022552/InformeResiduos2019.pdf/6ecdd830-e0a4-42c0-b2e2-cdc55460661d?version=1.0>.
- Jafari, A., & Sadeghian, P. (2023). Influence of biochar and recycled gypsum on the strength and microstructure of conventional and sustainable cementitious composites. *Construction and Building Materials*, 408, 133715. <https://doi.org/10.1016/j.conbuildmat.2023.133715>
- Jassam, T. M., Kien-Woh, K., Ng yang-zhi, J., Lau, B., & Yaseer, M. M. M. (2019). Novel cement curing technique by using controlled release of carbon dioxide coupled with nanosilica. *Construction and Building Materials*, 223, 692–704. <https://doi.org/10.1016/j.conbuildmat.2019.06.229>
- Kaur, H., Siddique, R., & Rajor, A. (2019). Influence of incinerated biomedical waste ash on the properties of concrete. *Construction and Building Materials*, 226, 428–441. <https://doi.org/10.1016/j.conbuildmat.2019.07.239>
- Khan, M., & Ali, M. (2019). Improvement in concrete behavior with fly ash, silica-fume and coconut fibres. *Construction and Building Materials*, 203, 174–187. <https://doi.org/10.1016/j.conbuildmat.2019.01.103>
- Khandelwal, H., Dhar, H., Thalla, A. K., & Kumar, S. (2019). Application of life cycle assessment in municipal solid waste management: A worldwide critical review. *Journal of Cleaner Production*, 209, 630–654. <https://doi.org/10.1016/j.jclepro.2018.10.233>
- Kocak, Y., & Nas, S. (2014). The effect of using fly ash on the strength and hydration characteristics of blended cements. *Construction and Building Materials*, 73, 25–32. <https://doi.org/10.1016/j.conbuildmat.2014.09.048>
- Kowalski, P. R., Kasina, M., & Michalik, M. (2016). Metallic elements fractionation in municipal solid waste incineration residues. *Energy Procedia*, 97, 31–36. <https://doi.org/10.1016/j.egypro.2016.10.013>
- Lenormand, T., Rozière, E., Loukili, A., & Staquet, S. (2015). Incorporation of treated municipal solid waste incineration electrostatic precipitator fly ash as partial replacement of Portland cement: Effect on early age behaviour and mechanical properties. *Construction and Building Materials*, 96, 256–269. <https://doi.org/10.1016/j.conbuildmat.2015.07.171>
- Margallo, M., Ziegler-Rodríguez, K., Vázquez-Rowe, I., Aldaco, R., Irabien, Á., & Kahhat, R. (2019). Enhancing waste management strategies in Latin America under a holistic environmental assessment perspective: A review for policy support. *Science of the Total Environment*, 689, 1255–1275. <https://doi.org/10.1016/j.scitotenv.2019.06.393>
- Martínez-López, C., Torres-Agredo, J., De Gutierrez, R. M., Mellado-Romero, A. M., Payá-Bernabeu, J., & Monzó-Balbuena, J. M. (2013). Use of leaching test to determine contaminant migration in mortars cement substituted with catalyst catalytic cracking residue (FCC). *DYNA (colombia)*, 80(181), 163–170.
- Medina, C., Sáez del Bosque, I. F., Frías, M., & Sánchez de Rojas, M. I. (2018). Design and characterisation of ternary cements containing rice husk ash and fly ash. *Construction and Building Materials*, 187, 65–76. <https://doi.org/10.1016/j.conbuildmat.2018.07.174>
- Memon, S. A., Javed, U., & Khushnood, R. A. (2019). Eco-friendly utilization of corncob ash as partial replacement of sand in concrete. *Construction and Building Materials*, 195, 165–177. <https://doi.org/10.1016/j.conbuildmat.2018.11.063>

- Methods, S. (2018, January 26). 2560D. Particle counting and size distribution (2017). *Standard Methods For the Examination of Water and Wastewater*. American Public Health Association. Retrieved February 1, 2020, from <https://www.standardmethods.org/doi/abs/https://doi.org/10.2105/SMWW.2882.032>
- Minambiente. (2022, May 17). Hoy no se habla de basura, sino de residuos que son insumos para productos: Minambiente. *Ministerio de Ambiente y Desarrollo Sostenible*. Retrieved November 28, 2022, from <https://www.minambiente.gov.co/asuntos-ambientales-sectorial-y-urbana/hoy-no-se-habla-de-basura-sino-de-residuos-que-son-insumos-para-productos-minambiente/>
- Moghaddam, F., Sirivivatnanon, V., & Vessalas, K. (2019). The effect of fly ash fineness on heat of hydration, microstructure, flow and compressive strength of blended cement pastes. *Case Studies in Construction Materials*, 10, 1–13. <https://doi.org/10.1016/j.cscm.2019.e00218>
- Morales, L. F., Herrera, K., López, J. E., Aguado, R., & Saldarriaga, J. F. (2023). Circular economy strategy for the valorization of fly ash as a substitute for cement in monoliths (resistance and reactivity evaluation). *Environmental Progress & Sustainable Energy*. <https://doi.org/10.1002/ep.14319>
- Morales, L. F., Herrera, K., López, J. E., & Saldarriaga, J. F. (2021). Use of biochar from rice husk pyrolysis: Assessment of reactivity in lime pastes. *Heliyon*, 7(11), e08423. <https://doi.org/10.1016/j.heliyon.2021.e08423>
- Nakanishi, E. Y., Frías, M., Santos, S. F., Rodrigues, M. S., Vigil de la Villa, R., Rodríguez, O., & Junior, H. S. (2016). Investigating the possible usage of elephant grass ash to manufacture the eco-friendly binary cements. *Journal of Cleaner Production*, 116, 236–243. <https://doi.org/10.1016/j.jclepro.2015.12.113>
- Nath, P., & Sarker, P. (2011). Effect of fly ash on the durability properties of high strength concrete. *Procedia Engineering*, 14, 1149–1156. <https://doi.org/10.1016/j.proeng.2011.07.144>
- Ordoñez-Ordoñez, E., Echeverry-Lopera, G., & Colorado-Lopera, H. (2019). Engineering and economics of the hazardous wastes in Colombia: The need for a circular economy model. *Informador Técnico*, 83(2), 155–173. <https://doi.org/10.23850/22565035.2041>
- Padilla, J. A., & Trujillo, J. C. (2018). Waste disposal and households' heterogeneity. Identifying factors shaping attitudes towards source-separated recycling in Bogotá, Colombia. *Waste Management*, 74, 16–33. <https://doi.org/10.1016/j.wasman.2017.11.052>
- Papamarkou, S., Christopoulos, D., Tsakiridis, P. E., Bartzas, G., & Tsakalakis, K. (2018). Vitrified medical wastes bottom ash in cement clinkerization. Microstructural, hydration and leaching characteristics. *Science of the Total Environment*, 635, 705–715. <https://doi.org/10.1016/j.scitotenv.2018.04.178>
- Pavliková, M., Zemanová, L., Pokorný, J., Záleská, M., Jankovský, O., Lojka, M., et al. (2018). Valorization of wood chips ash as an eco-friendly mineral admixture in mortar mix design. *Waste Management*, 80, 89–100. <https://doi.org/10.1016/j.wasman.2018.09.004>
- Prošek, Z., Nežerka, V., Hlůžek, R., Trejbal, J., Tesárek, P., & Karra'a, G. (2019). Role of lime, fly ash, and slag in cement pastes containing recycled concrete fines. *Construction and Building Materials*, 201, 702–714. <https://doi.org/10.1016/j.conbuildmat.2018.12.227>
- Qudoos, A., Kim, H. G., Atta-ur-Rehman, & Ryou, J.-S. (2018). Effect of mechanical processing on the pozzolanic efficiency and the microstructure development of wheat straw ash blended cement composites. *Construction and Building Materials*, 193, 481–490. <https://doi.org/10.1016/j.conbuildmat.2018.10.229>
- Rajamma, R., Ball, R. J., Tarelho, L. A. C., Allen, G. C., Labrincha, J. A., & Ferreira, V. M. (2009). Characterisation and use of biomass fly ash in cement-based materials. *Journal of Hazardous Materials*, 172(2), 1049–1060. <https://doi.org/10.1016/j.jhazmat.2009.07.109>
- Riahi, S., Nemat, A., Khodabandeh, A. R., & Baghshahi, S. (2020). The effect of mixing molar ratios and sand particles on microstructure and mechanical properties of metakaolin-based geopolymers. *Materials Chemistry and Physics*, 240, 122223. <https://doi.org/10.1016/j.matchemphys.2019.122223>
- Rodríguez-Fernández, M. C., Alonso, J. D., Montero, C., & Saldarriaga, J. F. (2020). Study of the effects of the addition of fly ash from carwash sludge in lime and cement pastes. *Sustainability*, 12(16), 6451. <https://doi.org/10.3390/su12166451>
- Saccani, A., Bignozzi, M. C., Barbieri, L., Lancellotti, I., & Bursi, E. (2017). Effect of the chemical composition of different types of recycled glass used as aggregates on the ASR performance of cement mortars. *Construction and Building Materials*, 154, 804–809. <https://doi.org/10.1016/j.conbuildmat.2017.08.011>
- Saikia, N., Mertens, G., Van Balen, K., Elsen, J., Van Gerven, T., & Vandecasteele, C. (2015). Pre-treatment of municipal solid waste incineration (MSWI) bottom ash for utilisation in cement mortar. *Construction and Building Materials*, 96, 76–85. <https://doi.org/10.1016/j.conbuildmat.2015.07.185>
- Saldarriaga, J. F., Gaviria, X., Gene, J. M., & Aguado, R. (2022). Improving circular economy by assessing the use of fly ash as a replacement of lime pastes reducing its environmental impact. *Process Safety and Environmental Protection*, 159, 1008–1018. <https://doi.org/10.1016/j.psep.2022.01.074>
- Sciences, T. I.-A. N. of A. of. (2019). Calidad del agua en las Américas. Riesgos y oportunidades. (M. Roldan, Gabriel; Tundisi, Jose; Jimenez, Blanca; Vammen, Katherine; Vauz, Henry; Gonzalez, Ernesto; Doria,

- Ed.). México D.F: IANAS. Retrieved March 14, 2020, from <https://www.ianas.org/images/books/wb9d.pdf>
- Sharma, R. (2018). Laboratory study on sustainable use of cement–fly ash–polypropylene fiber-stabilized dredged material. *Environment, Development and Sustainability*, 20(5), 2139–2159. <https://doi.org/10.1007/s10668-017-9982-0>
- Siddique, R. (2013). Compressive strength, water absorption, sorptivity, abrasion resistance and permeability of self-compacting concrete containing coal bottom ash. *Construction and Building Materials*, 47, 1444–1450. <https://doi.org/10.1016/j.conbuildmat.2013.06.081>
- Siddique, R., Aggarwal, P., & Aggarwal, Y. (2012). Influence of water/powder ratio on strength properties of self-compacting concrete containing coal fly ash and bottom ash. *Construction and Building Materials*, 29, 73–81. <https://doi.org/10.1016/j.conbuildmat.2011.10.035>
- Song, H., Jeong, Y., Bae, S., Jun, Y., Yoon, S., & Oh, J. E. (2018). A study of thermal decomposition of phases in cementitious systems using HT-XRD and TG. *Construction and Building Materials*, 169, 648–661. <https://doi.org/10.1016/j.conbuildmat.2018.03.001>
- Soyinka, O. A., Wadu, M. J., Lebunu Hewage, U. W. A., & Oladinrin, T. O. (2023). Scientometric review of construction demolition waste management: A global sustainability perspective. *Environment, Development and Sustainability*, 25(10), 10533–10565. <https://doi.org/10.1007/s10668-022-02537-7>
- Stiernström, S., Enell, A., Wik, O., Borg, H., & Breitholtz, M. (2014). An ecotoxicological evaluation of aged bottom ash for use in constructions. *Waste Management*, 34(1), 86–92. <https://doi.org/10.1016/j.wasman.2013.10.003>
- Sua-iam, G., & Makul, N. (2013). Use of increasing amounts of bagasse ash waste to produce self-compacting concrete by adding limestone powder waste. *Journal of Cleaner Production*, 57, 308–319. <https://doi.org/10.1016/j.jclepro.2013.06.009>
- Tang, S. W., Cai, X. H., He, Z., Shao, H. Y., Li, Z. J., & Chen, E. (2016). Hydration process of fly ash blended cement pastes by impedance measurement. *Construction and Building Materials*, 113, 939–950. <https://doi.org/10.1016/j.conbuildmat.2016.03.141>
- Tantawy, M. A., El-Roudi, A. M., & Salem, A. A. (2012). Immobilization of Cr(VI) in bagasse ash blended cement pastes. *Construction and Building Materials*, 30, 218–223. <https://doi.org/10.1016/j.conbuildmat.2011.12.016>
- Teixeira, E. R., Camões, A., Branco, F. G., Aguiar, J. B., & Figueiro, R. (2019). Recycling of biomass and coal fly ash as cement replacement material and its effect on hydration and carbonation of concrete. *Waste Management*, 94, 39–48. <https://doi.org/10.1016/j.wasman.2019.05.044>
- Termkhajornkit, P., Nawa, T., Yamashiro, Y., & Saito, T. (2009). Self-healing ability of fly ash–cement systems. *Cement and Concrete Composites*, 31(3), 195–203. <https://doi.org/10.1016/j.cemconcomp.2008.12.009>
- Toniolo, N., & Boccaccini, A. R. (2017). Fly ash-based geopolymers containing added silicate waste: A review. *Ceramics International*, 43(17), 14545–14551. <https://doi.org/10.1016/j.ceramint.2017.07.221>
- US EPA, O. (2015). SW-846 Test Method 1312: Synthetic precipitation leaching procedure. *US EPA*. Retrieved from <https://www.epa.gov/hw-sw846/sw-846-test-method-1312-synthetic-precipitation-leaching-procedure>
- US EPA, O. R. D. (2019). EPA Method 3015A: Microwave assisted acid digestion of aqueous samples and extracts. *US EPA*. Retrieved February 15, 2020, from <https://www.epa.gov/esam/epa-method-3015a-micro-wave-assisted-acid-digestion-aqueous-samples-and-extracts>
- Velázquez, S., Monzó, J., Borrachero, M. V., Soriano, L., & Payá, J. (2016). Evaluation of the pozzolanic activity of spent FCC catalyst/fly ash mixtures in Portland cement pastes. *Thermochimica Acta*, 632, 29–36. <https://doi.org/10.1016/j.tca.2016.03.011>
- Wang, X., Yu, Y., Zou, F., Luo, H., Zhou, Z., Zhu, J., et al. (2023). High performance C-A-S-H seeds from fly ash-carbide slag for activating lithium slag towards a low carbon binder. *Journal of Environmental Management*, 345, 118658. <https://doi.org/10.1016/j.jenvman.2023.118658>
- Wang, Y., Shao, Y., Matovic, M. D., & Whalen, J. K. (2014). Recycling of switchgrass combustion ash in cement: Characteristics and pozzolanic activity with chemical accelerators. *Construction and Building Materials*, 73, 472–478. <https://doi.org/10.1016/j.conbuildmat.2014.09.114>
- Xu, J. Z., Zhou, Y. L., Chang, Q., & Qu, H. Q. (2006). Study on the factors of affecting the immobilization of heavy metals in fly ash-based geopolymers. *Materials Letters*, 60(6), 820–822. <https://doi.org/10.1016/j.matlet.2005.10.019>
- Yang, Z., Tian, S., Liu, L., Wang, X., & Zhang, Z. (2018). Recycling ground MSWI bottom ash in cement composites: Long-term environmental impacts. *Waste Management*, 78, 841–848. <https://doi.org/10.1016/j.wasman.2018.07.002>
- Yusuf, A. A., Peter, O., Hassan, A. S., Tunji, L. A., Oyagbola, I. A., Mustafa, M. M., & Yusuf, D. A. (2019). Municipality solid waste management system for Mukono District, Uganda. *Procedia Manufacturing*, 35, 613–622. <https://doi.org/10.1016/j.promfg.2019.06.003>

Publisher's Note Springer Nature remains neutral with regard to jurisdictional claims in published maps and institutional affiliations.